Adsorption and desorption of uranium(VI) onto humic acids derived from uranium-enriched lignites

Yangyang Zhang, Yilian Li, Yu Ning, Danqing Liu, Peng Tang, Zhe Yang, Yu Lu and Xianbo Wang

ABSTRACT

Humic acids (HAs) were extracted and characterized from three kinds of uranium-enriched lignites from Yunnan province, China. Batch experiments were used to study the adsorption and desorption behavior of uranium (VI) onto these HAs and a commercial HA. The results showed that the optimum pH level at which all the HAs adsorbed uranium(VI) ranged from 5 to 8. The high uranium content of the HAs was released into the solution at the pH values between 1 and 3; when the HA dosage was 2.5 g L^{-1}, the maximum concentration of uranium was 44.14 μg L^{-1}. This shows that HAs derived from uranium-enriched lignites may present a potential environmental risk when used in acidic conditions. The experimental data were found to comply with the pseudo-second-order kinetic model, and the adsorption isotherms fit the Langmuir and Freundlich models well. The desorption experiments revealed that the sorption mechanism was controlled by the complex interactions between the organic ligands of the HAs and uranium(VI). The uranium present in the HAs may not affect the adsorption capacity of the uranium(VI), but the carboxylic and phenolic hydroxyl groups in the HAs play a significant role in controlling the adsorption capacity.

Key words | adsorption, humic acid, lignite, uranium

Yangyang Zhang
Yilian Li (corresponding author)
Yu Ning
Danqing Liu
Peng Tang
Zhe Yang
Yu Lu
Xianbo Wang
School of Environmental Studies,
China University of Geosciences,
Wuhan, Hubei Province 430074,
China
E-mail: *yl.li@cug.edu.cn*

INTRODUCTION

Uranium is a natural radioactive trace element existing in rocks, soils, and coals. Due to human activities such as mining of U-enriched ores, nuclear fuel processing and coal combustion (Jing *et al.* 2015; Zhang *et al.* 2016), the occurrence of uranium in soil and groundwater is a serious environmental problem. The mobility and toxicity of uranium in the aquatic environment depend on its speciation. Under oxic conditions, U(VI) is the main oxidation state of uranium, present in natural water systems primarily as the uranyl cation (UO_2^{2+}) or as uranyl–hydroxide–carbonate complexes. Under anoxic conditions, U(VI) can be reduced to U(IV) by inorganic reductants. The mobility and biotoxicity of U(VI) is much higher than U(IV). A number of recent studies have focused on understanding the interaction between U(VI) and water (Sun *et al.* 2016; Wang *et al.* 2017a), yet an eco-friendly and practical technology for the removal of U(VI) from aqueous solution has not been developed.

Humic acid (HA) is a natural product that is ubiquitous in soils and natural waters, and HA can control trace element cycling and pollutant mobility. HA is a colloid having various functional groups, such as carboxylic, phenolic hydroxyl, alcoholic hydroxyl and carbonyl, which have shown remarkable effect in removing heavy metals. Because HA is an eco-friendly substance, the use of it would not introduce foreign materials into an engineered reaction system; its utilization as an adsorbing material has been a topic of intense research in recent years. Khalili *et al.* (2017) extracted HA from the Azraq soil and investigated the sorption properties of U(VI). The result of the column experiment showed that HA has good U(VI) uptake properties. HA occurs not only in soils, natural waters, and sediments but also in lignite and bituminous coal. Lignite is a low-rank coal with large amounts of humic and fulvic acids, and due to its low calorific value, high ash content and high content of moisture, lignite is mainly used as a fertilizer or source of HA and fulvic acid due to the high content of organic oxygen (Ciarkowska *et al.* 2017; Wang *et al.* 2017b). Many researchers have focused on the adsorption characteristics of HA derived from lignite. Wang *et al.*

doi: 10.2166/wst.2017.608

(2017b) investigated the characteristic of the HAs from lignite, and they showed that it was rich in hydroxyl and carboxyl groups. Pehlivan & Arslan (2006) appraised the removal of heavy metals with HAs derived from lignites, and HAs proved to be a useful adsorbent for Zn(II) and Cd(II). However, research on the interactions between U(VI) and HA from lignite is limited.

Due to the lignite having abundant organic matter (OM), it can be a biogeochemical trap for uranium. Uranium can co-precipitate with OM and lignite may even contain up to several hundred milligrams of U per kilogram (Hou *et al.* 2017). The uranium content of lignite in individual regions of China is abnormally high; the main deposits of the uranium-enriched coals in China are in the Yunnan province. The concentration of uranium in the Late Permian coals in the Yunnan province is 200 mg kg^{-1} (Yang 2007), while the uranium concentration of coals in the Yanshan coalfield of Yunnan Province is 153 mg kg^{-1} (Dai *et al.* 2008). The environmental risks of uranium-enriched lignite cannot be overlooked. As lignite is an important source of HA, research into U(VI) adsorption onto HAs derived from lignites, especially the uranium-enriched lignites, is needed.

In our present investigation, we have isolated HAs from three kinds of uranium-enriched lignites in the Yunnan province, China and characterized it by Fourier transform infrared spectroscopy (FTIR), element analysis, determination of HAs acidity and UV–visible (UV-Vis) spectroscopy. The adsorption behavior of uranium on these HAs and a commercial HA were investigated, as well as the effect of initial pH, adsorption kinetics and isotherms to explore whether the high content of uranium present in the HAs can affect the adsorption and reaction system; desorption by two eluting agents (NH_4Ac and EDTA) was studied to understand the nature of adsorption mechanisms.

MATERIALS AND METHODS

Chemicals

All the reagents were analytical grade and purchased from Sinopharm Chemical Reagent Co. (Shanghai, China). The U solution was prepared with $UO_2(NO_3)_2{\cdot}6H_2O$ in deionized water (18.25 M cm^{-1}, total organic carbon ≤ 10 μg L^{-1}) (UPT-I, Ulupure, China). All the glassware, polyethylene tubes, and Teflon beakers were soaked in a 20% (V/V) HNO_3 solution for 48 h and then washed with deionized water before and after each experiment to avoid the binding to metals. The pH was adjusted by adding moderate amounts of hydrochloric acid or sodium hydroxide using a pH meter (PB-10, Sartorius), which was calibrated with different buffers (pH = 1.68, 4.00, 6.86, 9.18).

Preparation of HAs

Three samples of HA used in this study were extracted from three different lignite mines respectively, which were the Mengwang coal mine (MW), the Dazhai coal mine (DZ) and the Huimei coal mine (HM). All of these mines are located in the Lincang city, Yunnan province, China. The uranium content in the lignites was determined by the method from Dai *et al.* (2011); the uranium concentration of the lignites from above-mentioned mines is 101.22, 60.86 and 16.71 mg kg^{-1}, respectively. A commercial sample of HA (C-HA) was obtained from the Tianjin Guangfu fine chemical research institute. The extraction of the three HA samples (MW-HA, DZ-HA, and HM-HA) was conducted with the alkali extraction method (Cihlář *et al.* 2016). One hundred grams of the air-dried lignite sample was ground to grain size <0.2 mm and homogenized. Then the lignite sample was mixed with 0.5 mol L^{-1} NaOH and 0.1 mol L^{-1} $Na_4P_2O_7{\cdot}10H_2O$ (1:1) at a volume ratio of 10:1 (mass/V) and shaken for 3 h. Then, the mixture was centrifuged at 5,000 rpm for 20 min, after which 6 mol L^{-1} HCl was added to the supernatant until obtaining the pH of 1 to precipitate the HAs. Afterwards, 0.5% HCl-HF solution was added to precipitated HAs for 24 h to eliminate the inorganic impurities and then centrifuged at 5,000 rpm for 20 min. Obtained HAs were repeatedly washed until chloride-free and freeze-dried. All the HA samples were finely milled and used in the form of humic powder.

Chemical characterization of HAs

The contents of C, H, N, S, and O in the HAs were measured using an elemental analyzer (Vario MACRO). The ash content was determined by combustion of 200.0 mg of HAs in a muffle furnace at 850 °C for 2 h. HAs were acid digested using a conventional HF-HNO_3-$HClO_4$ digestion procedure on an electrothermal plate. The concentration of the metallic elements was measured with inductively coupled plasma mass emission spectroscopy (ICP-MS) (ELAN DRC-II, PerkinElmer SCIEX., USA). The internal standard is Rh (10 μg L^{-1}) in 3% (V/V) HNO_3. The accuracy of the duplicate analyses was within ±5%.

The total acidic groups, the carboxyls, and the phenol-hydroxyls in the HAs were measured by conventional methods (Klučáková & Pekař 2008). Absorbance was

measured at 465 nm and 665 nm (E4 and E6 respectively), for a 0.2 g L^{-1} solution of HAs at pH 6.5, and then the E4/E6 ratio was calculated.

The chemical compositions of the four HA samples were characterized by FTIR spectroscopy (Nicolet 6700, Thermo Corp., USA). HA samples were dried at 45 °C for 3 hours in the oven, then prepared by mixing with KBr powder (1%, m/m) and pressing the mixture into a sheer slice. The FTIR spectra were scanned in the transmission mode from 4,000 to 400 cm^{-1}, and the FTIR data were analyzed by OMNIC 8.2.0.

Adsorption experiments

The adsorption procedures were performed in a continuously stirred polyethylene tube containing a solution of the U(VI) with single factor analysis method. We firstly prepared 20 mL U(VI) solution with concentration of 100 μg L^{-1} in the 50 mL polyethylene tube and adjusted the pH to 1–10. One milligram of HAs was then added to the U(VI) solution and shaken for 8 h at a shaking rate of 100 rpm. The adsorption isotherms were investigated using similar conditions at the pH of 5 using various initial U(VI) concentrations (25–300 μg L^{-1}) and different temperatures (25, 45 °C). At the end of the agitation, the suspensions were centrifuged at 4,000 rpm for 5 min and then passed through a 0.22 μm membrane filter. Afterward, the solutions were dissolved with 3% (V/V) HNO_3 to analyze the residual concentration of U(VI) as described before with ICP-MS. The U(VI) removal rate was calculated by Equation (1):

$$\text{U(VI) removal } \% = \frac{C_0 - C_e}{C_0} \times 100 \quad (1)$$

where C_0 is the initial concentration of U(VI) (mg L^{-1}), C_e is the equilibrium concentration of U(VI) (mg L^{-1}). The amount of U(VI) ion adsorbed by the unit amount of HAs was calculated with the Equation (2):

$$q_e = \frac{(C_0 - C_e) \times V}{m} \quad (2)$$

where q_e is the sorption capacity (mg g^{-1}), V is the solution volume (L), and m is the amount of HA adsorbent (g). Blank tests showed that the sorption of U(VI) on the centrifuge tube and the solubility of HAs were exiguous. All the adsorption experiments were repeated in duplicate under the identical conditions; the relative standard error of was within 5%.

Adsorption kinetics models

For modeling the kinetic parameters of the U(VI) adsorption by the HAs, the first-order equation (Equation (3)), pseudo-second-order equation (Equation (4)), and intraparticle diffusion model (Equation (5)) have been used.

The three models can be expressed as:

$$\ln(q_e - q_t) = \ln q_e - k_1 t \quad (3)$$

$$\frac{t}{q_t} = \frac{1}{k_2 q_e^2} + \frac{t}{q_e} \quad (4)$$

$$q_t = k_3 t^{0.5} + C \quad (5)$$

where q_t (mg g^{-1}) is the amount of adsorbate absorbed at time t (min), q_e is the sorption capacity (mg g^{-1}) at equilibrium, k_1 (min^{-1}) and k_2 (g mg^{-1} min^{-1}) are the rate constant for first-order model and pseudo-second-order model, respectively. k_3 is the is the rate constant of intraparticle diffusion model, C is a constant.

Adsorption isotherm models

The Langmuir model and the Freundlich model were used for analyzing the experimental sorption equilibrium data. The Langmuir model is based on the presumption that the adsorbent surface is uniform with a finite number of identical sites, and only a monolayer is formed during sorption onto a solid surface. The Freundlich model is an empirical equation usually applicable to non-ideal sorption on an irregular surface as well as multilayer sorption. These two models are expressed as:

$$q_e = \frac{Q_m K_L C_e}{1 + K_L C_e} \quad (6)$$

$$q_e = K_F C_e^{1/n} \quad (7)$$

where Q_m is the saturated adsorption amount of U(VI) reflecting a complete monolayer (mg g^{-1}), K_L is a binding constant (L mg^{-1}); K_F is the amount of U(VI) adsorbed by HA, n is the intensity of adsorption.

Desorption experiments

NH_4Ac and EDTA were chosen to study the desorption of U(VI) from the HAs. Twenty milligrams of HAs were

added into 20 mL of 10 mg L^{-1} U(VI) solution in 50 mL conical flasks. The desorption experiments were maintained at pH of 5 and temperature of 25 °C, and shaking for 24 h at a shaking rate of 100 rpm to ensure approaching equilibrium. The maximum sorption capacity of the MW-HA, DZ-HA, HM-HA, and C-HA were 3.96, 1.51, 6.02, and 9.50 mg g^{-1}, respectively. After centrifugation and filtration, the HA samples were washed with deionized water and freeze-dried. Two milligrams of solid samples were added into 50 mL of the eluting solutions with varying concentrations and shaken for 8 h. The desorption amount can be determined from the concentration of the U(VI) in the solution.

RESULTS AND DISCUSSION

Basic characteristics of HAs

The elemental compositions of the HAs and the ratios of O/C and H/C are given in Tables 1 and 2. The results show that the C-HA contains more oxygen compared with the MW-HA, DZ-HA, and HM-HA. The O/C ratio reveals the hydrophilicity degree of the HAs. A higher value of this ratio indicates that the HA may have a higher content of oxygen functional groups (e.g. -COOH, -OH) (Cihlář *et al.* 2014). This is reflected in the determination of HAs acidity as shown in Table 3, in which the total of the acidic groups of C-HA is higher than the other three kinds of HAs, while the total of the acidic groups of DZ-HA is the lowest among all of the HAs. The decrease of the total acidic groups is in the order of C-HA > HM-HA > MW-HA > DZ-HA, which has a close correlation relationship with O/C ratio. E4/E6 ratio is associated with the degree of humification and the molecular weight of the HAs. High E4/E6 ratio indicates less degree of aromaticity and lower molecular weight. The decrease of E4/E6 ratio, as shown in Table 3 in the order of DZ-HA > MW-HA > HM-HA > C-HA, is an indication of increasing humification, aromaticity and molecular weight.

FTIR spectroscopy of the HAs shown in Figure 1 indicates that all the samples show a broad band at 3,420 cm^{-1} which is assigned to the O-H vibration of the carboxylic and alcoholic groups (Pehlivan & Arslan 2006). The weak absorption around 2,350 cm^{-1} is assigned to the hydrogen bonded groups (O-H stretching of COOH) (Ghabbour *et al.* 2004). The weak band at 1,440 cm^{-1} in the MW-HA, DZ-HA and HM-HA is attributed to the O-H deformation or C = O stretching of the phenolic groups (Khalili & Al-Banna 2015). The band at 1,620 cm^{-1} is assigned to the aromatic carbonyl and carbonyl motion in the carboxyl groups. The intensity of band 1,620 cm^{-1} shows that the C-HA and HM-HA contain more carboxylic acids than the other samples. The band at 1,620 cm^{-1} is also a measure of the humification. The higher intensity of 1,620 cm^{-1} observed in the C-HA and HM-HA further confirms a higher humification than in the other samples. The band at 1,170 cm^{-1} is assigned to the C-O vibration of tertiary alcohol. Two bands at 985 and 732 cm^{-1} in the MW-HA, DZ-HA and HM-HA are due to the bending of aromatic C-H. FTIR spectra of the HA samples indicates that the amount of carboxyl functional groups in the C-HA and HM-HA may be higher than the MW-HA and DZ-HA; the content of functional groups shown in Table 3 also confirms this.

Effect of initial pH

The effect of the initial pH on the U(VI) sorption is shown in Figure 2. The sorption of U(VI) on the four different HAs increases abruptly with the increase of pH when the pH is less than 3, then achieves a peak and remains constant at pH of 5–8. When pH > 8, the removal percentage decreased. The pH of the U(VI) solution affects the species distributions of U(VI), and the surface charge of HAs. These factors affect the adsorption mechanism and the U(VI) removal percentage. The uranium removal percentage of the C-HA is higher than the HAs derived from lignites. This indicates that the functional groups of the HAs play a major role in

Table 1 | Contents of the organic elements in the HAs and their respective ratios

Sample	C[a]	H[a]	O[a,b]	N[a]	S[a]	H/C	O/C	w[c]	Ash[c]
MW-HA	60.33	5.53	32.97	0.68	0.49	1.10	0.41	7.2	5.12
DZ-HA	65.30	6.02	28.01	0.52	0.15	1.11	0.32	6.3	8.15
HM-HA	59.40	5.37	34.10	0.62	0.51	1.08	0.43	7.9	4.36
C-HA	54.42	4.43	39.67	1.06	0.42	0.98	0.55	4.6	2.69

Note: [a]dry sample; [b]calculated by difference; [c]moisture content and ash are in wt.%; C, H, O, N and S are in wt.%; H/C, O/C are in at.%.

Table 2 | Elemental composition of HAs

Element	MW-HA	DZ-HA	HM-HA	C-HA
As	76.48	174.31	77.77	117.34
V	79.31	30.31	64.92	13.08
Mn	60.66	119.37	137.35	113.97
Co	1.80	11.37	12.25	63.42
Cu	5.54	31.09	59.09	78.45
Rb	5.12	15.06	63.04	46.55
Cd	0.94	4.18	4.07	7.51
Ba	141.90	388.41	505.93	377.05
Pb	21.60	82.80	40.61	46.73
Cs	3.83	20.46	26.38	16.29
Ni	13.84	53.34	40.91	35.08
U	66.91	19.92	7.53	0.80

Note: all the elements are in mg kg^{-1}.

Table 3 | Content of the functional group and E4/E6

	Content of the functional group/mmol g^{-1}			
Sample	Total acidic groups	Carboxyls	Phenol-hydroxyls	E4/E6
MW-HA	1.72	0.72	1.00	5.08
DZ-HA	1.02	0.48	0.54	5.91
HM-HA	2.52	1.58	0.94	4.42
C-HA	3.34	2.02	1.32	3.65

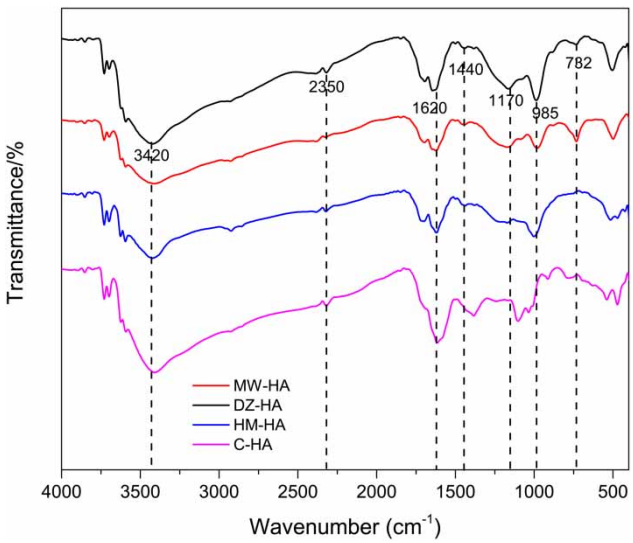

Figure 1 | Comparison of FTIR spectra for HA samples.

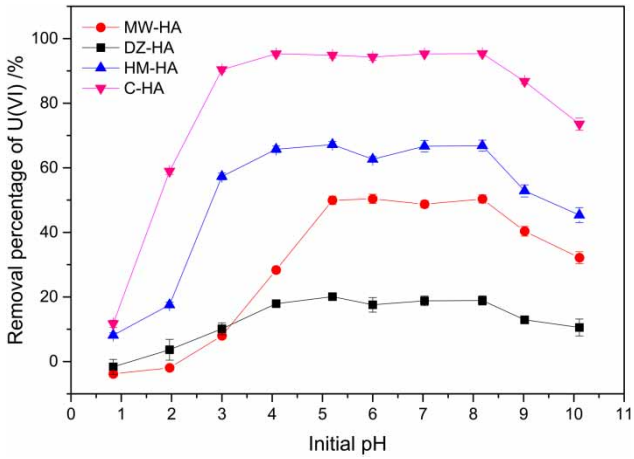

Figure 2 | Effect of pH on U(VI) adsorption (T = 25 °C, $C_{U(initial)}$ = 100 μg L^{-1}, ionic strength = 0 mol L^{-1}).

the adsorption of the U(VI), which may be because the C-HA has a higher content of carboxylic group (2.02 mmol g^{-1}) and phenol-hydroxyl group (1.32 mmol g^{-1}) than the other HAs and therefore binds more U(VI).

The U(VI) species are present in the forms of UO_2^{2+}, $UO_2(OH)^+$, $(UO_2)_3(OH)_5^+$, $UO_2(OH)_3^-$ and $UO_2(OH)_4^{2-}$ at different pH values, and the U(VI) species change from positively charged to negatively charged with pH ranging from 1 to 14, as simulated by Visual MINTEQ 3.1 in Figure 3. When pH < 5, positively charged UO_2^{2+} exists as the predominant species (≥70%), while $UO_2(OH)^+$ is less than 29%. At pH of 6, $UO_2(OH)^+$ is the predominant species (≥62%), and the amount of $(UO_2)_3(OH)_5^+$ increases. At pH of 6–8, a mixture of species of $UO_2(OH)^+$ and $(UO_2)_3(OH)_5^+$ is observed. Negatively

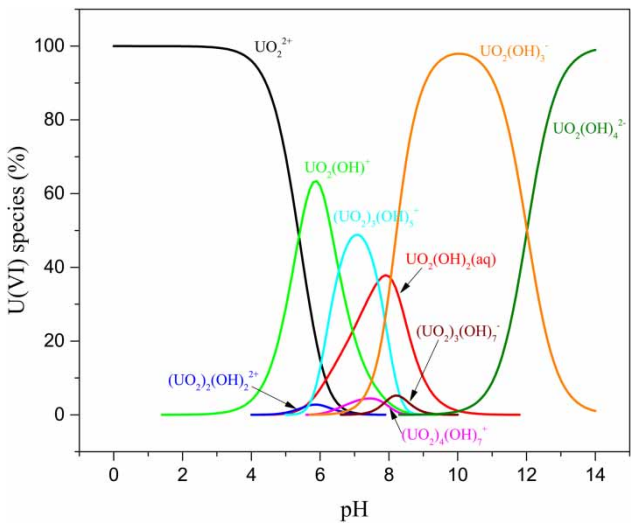

Figure 3 | Effect of pH on speciation of U(VI) (T = 25 °C, $C_{[U(initial)]}$ = 100 μg L^{-1}, ionic strength = 0 mol L^{-1}).

charged species of $UO_2(OH)_3^-$ and $UO_2(OH)_4^{2-}$ become dominant species at pH ≥ 9. Yue *et al.* (2009) found that slight dissolution of the HA raised the negative charges on the surface in neutral solution, the zeta potential of HA was about −35 mV, and the uranium cations could easily adsorb on the surface of HA. However, with the increasing of pH (pH > 8), it is difficult for the negatively charged species of uranium to adsorb onto the negatively charged surface of HA, which is the major cause for U(VI) removal percentage decreasing at higher pH values.

HAs are highly functionalized, the amount of H^+ released by HAs is controlled by the number of functional groups and the system pH. The low pH values (≤4.0) inhibit the functional groups' release of H^+; however, the plentiful H^+ in solution restrains the hydrolysis of HAs, leading to the decrease of negative charges on the HAs. Li *et al.* (2010) found that the increased removal rates of the metal ions were mainly ascribed to the ion-exchange effect between metal ions and H^+ as the pH increases. Figure 4 shows the final pH of U(VI) solution. It can be observed that the decrease of the final pH in the HAs was attributed to the release of H^+; this process can be expressed as (Li *et al.* 2015):

$$M^{n+} + HA \rightarrow MA^{n-1} + H^+ \quad (8)$$

$$MA^{n-1} + HA \rightarrow MA^{n-2} + H^+ \quad (9)$$

$$M^{n+} + H_mA \rightarrow MA^{n-m} + mH^+ \quad (10)$$

where M is metal ion and MA is metal–HA complex.

However, the pH reduction range of the four kinds of HAs are different. When the initial pH value is between 5 and 10, the final pH of C-HA is higher than that of the other three HAs. It can be assumed that an adsorption process without the release of H^+ may occur (Adamczuk & Kołodyńska 2015):

$$2 - NH_2 + M^{2+} \rightarrow (-NH_2)_2M \quad (11)$$

At pH 1, the U(VI) removal percentage of the MW-HA and DZ-HA were −3.82% and −1.66%. We assume that the uranium present in the HAs can release to the solution at the lower pH values. To verify this assumption, we prepared a 20 mL solution of the HAs at various concentrations (0.05, 0.5, 1.25 and 2.5 g L^{-1}) in 50 mL polyethylene tube and adjusted pH to 1–10, which was then shaken for 8 h at a shaking rate of 100 rpm. The effect of pH on uranium release to the solution is shown in Figure 5. The concentration of uranium released from the HAs increased with the increasing of HAs concentration at pH of 1–3. With the reduction of hydrogen ion concentration in the solutions, the release processes were not obvious in the neutral and alkaline conditions. The concentrations of uranium in the MW-HA, DZ-HA, HM-HA, and C-HA were 66.91, 19.92, 7.53, and 0.80 mg kg^{-1}, respectively. When the HAs dosage was 2.5 g L^{-1}, the release amounts of uranium of these HAs were 44.14, 16.20, 3.71 and 0.25 μg L^{-1} at pH 1.0. There was a positive correlation between the release amount and uranium content in the HAs. The H^+ in the solution may replace the uranium ions in the HAs. With limited H^+ concentration, the release amount of uranium did not multiply with the rise of HAs concentration. The utilization of HAs derived from lignite in the environment has been reported (Cihlář *et al.* 2014), and many previous studies demonstrated that the HAs can change both the chemical and the physical characteristics of the metal ions and affected their bioactivity and mobility (Kautenburger *et al.* 2017). In 2011, the World Health Organization regulated the provisional guideline value of uranium (<30 μg L^{-1}) in drinking water (World Health Organization 2011). However, in this study, the HAs derived from uranium-enriched lignites could release the uranium into the solutions under acidic conditions, with maximum concentration of U to be 44.14 μg L^{-1}. Before the large-scale application of HAs derived from uranium-enriched lignites, the environmental risks need further evaluation.

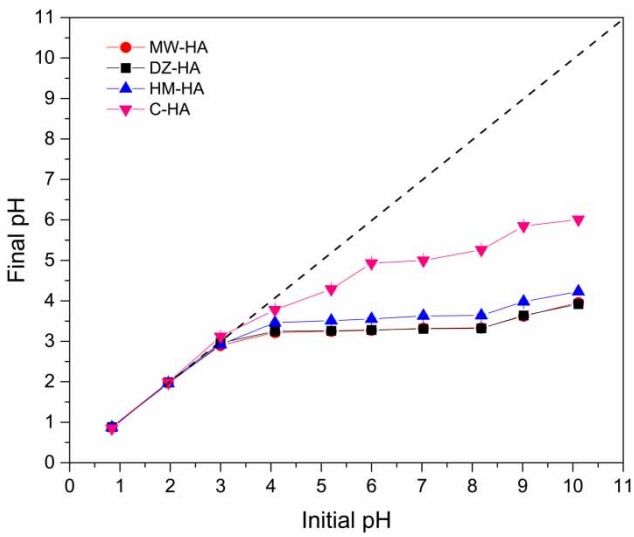

Figure 4 | The final pH of U(VI) solution.

Adsorption kinetics

Figure 6 plots the q_t variation versus time for the U(VI) onto the HAs for various C_0 (50, 100 and 200 μg/L) at 25 °C, pH 5. We conclude from this figure that the U(VI) sorption by

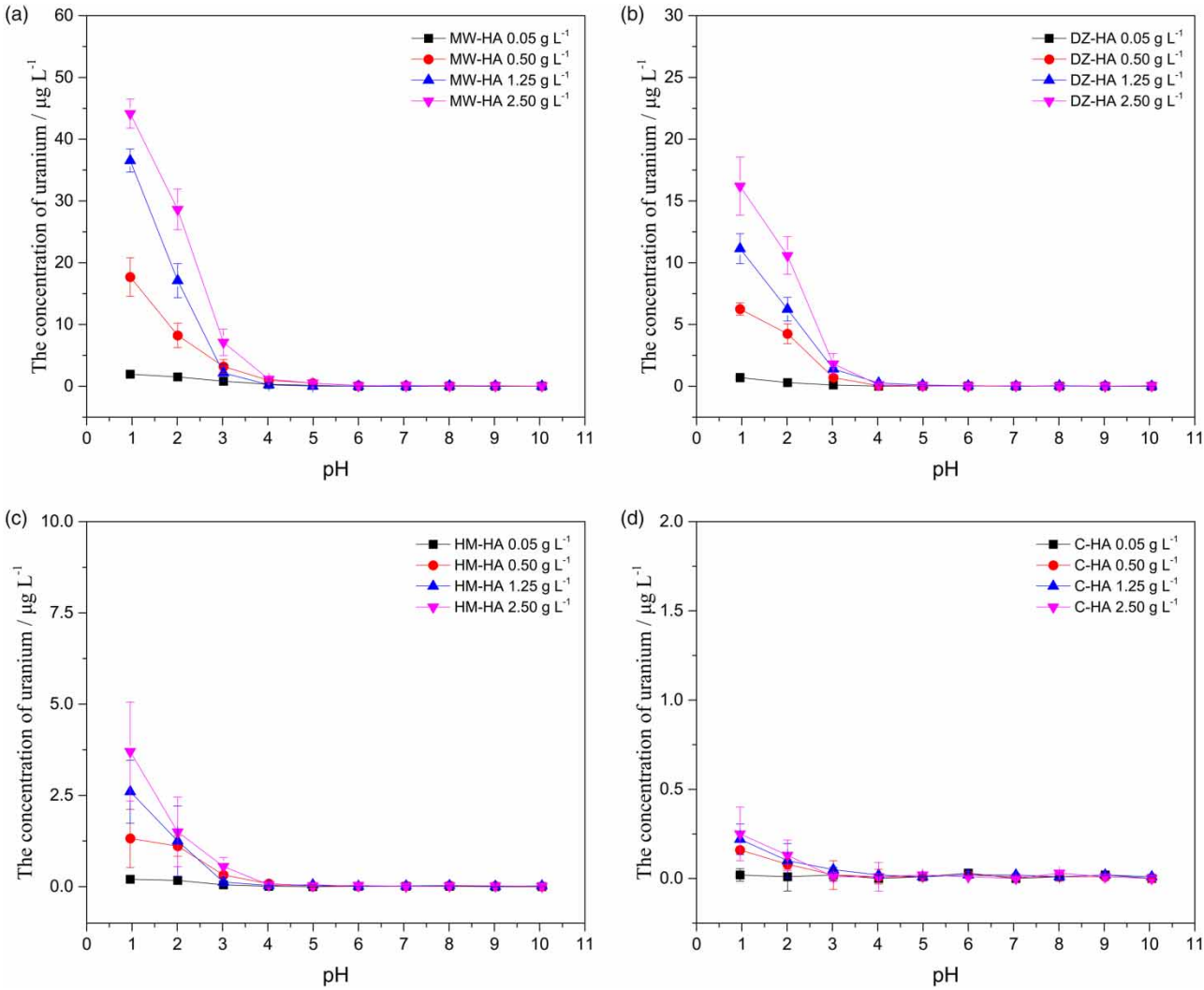

Figure 5 | Effect of pH on uranium release from (a) MW-HA, (b) DZ-HA, (c) HM-HA and (d) C-HA (T = 25 °C, pH = 1–10, ionic strength = 0 mol L^{-1}).

the HAs from the lignites needs about 6 h to reach equilibrium; the U(VI) sorption by the C-HA needs about 4 h to reach equilibrium. The value of q_t increased rapidly during the beginning of the adsorption, then the increasing rate slows down, and the external mass transfer diffusion is not the control mechanism of the adsorption process.

To investigate the adsorption mechanism and reaction order, the kinetics data were fitted to three kinetic models. The kinetic rate parameters, the correlation coefficients, and calculated and experimental q_e values are listed in Table 4. According to the intraparticle diffusion model, if the value of C is 0, the intraparticle diffusion is the rate limiting step in the adsorption; if not, the adsorption process is controlled by other adsorption stages. Li *et al.* (2010) suggested that the heavy metals adsorbed by the HA may include three stages; the first stage is the external sorption, the second stage is attributed to intraparticle diffusion, the last one is equilibrium stage. In this study, intraparticle diffusion is not the main mechanism of the adsorption. As seen from Table 4, the pseudo-second-order model could well simulate the data, among which the r^2 of the pseudo-second-order model is higher than that for the first-order model and the intraparticle diffusion model. This illustrates that the pseudo-second-order model could describe the adsorption kinetics of U(VI) onto the HAs.

The sorption capacity calculated from the pseudo-second-order equation (q_{e2}(cal)) is much more close to the experimental value, q_e(exp), than is the first-order equation. It also indicates that the pseudo-second-order model is more suitable for the adsorption system. We find that q_e(exp) increases with the increase of C_0. The increase of U(VI) concentration could provide more

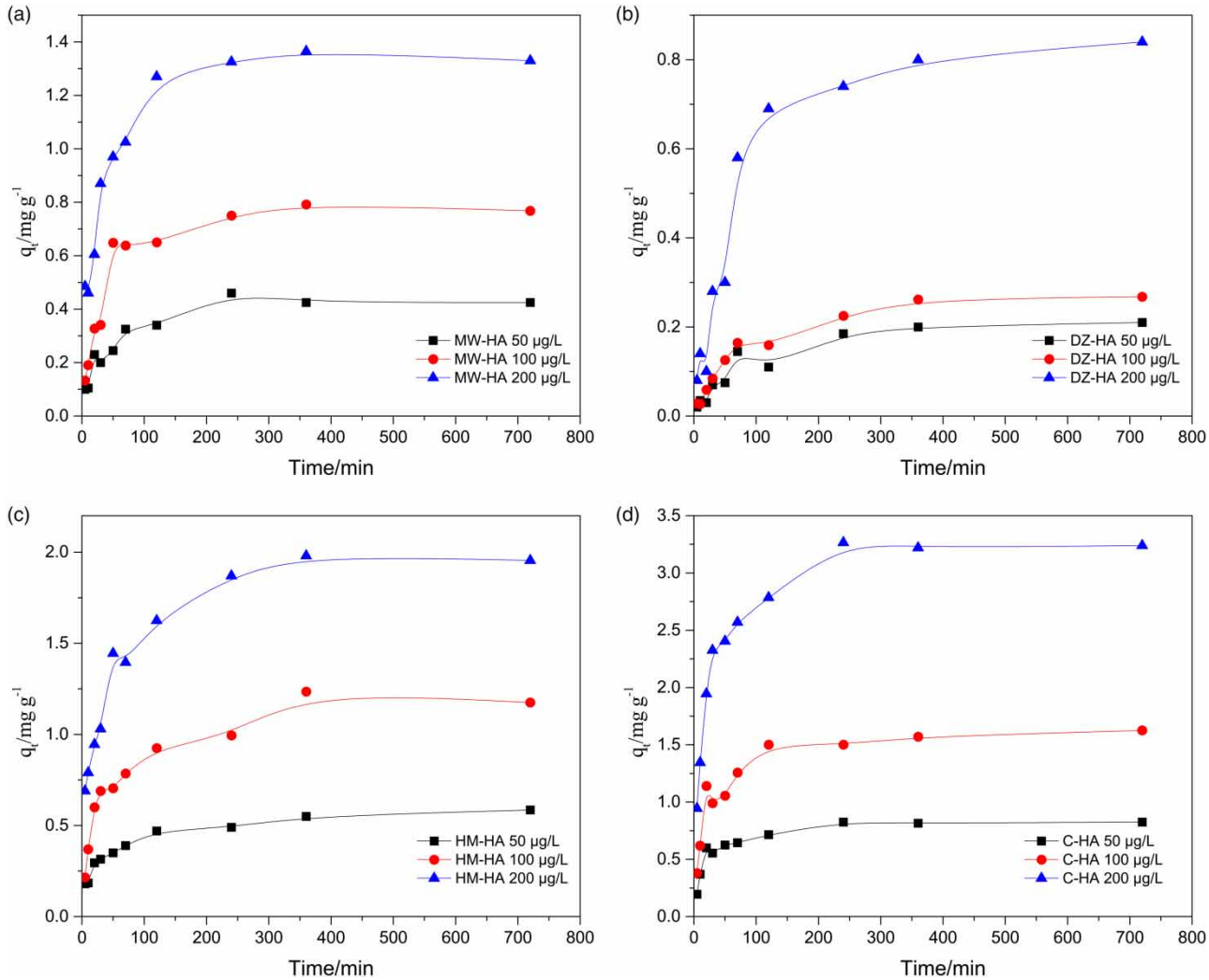

Figure 6 | Effect of initial concentration on U(VI) adsorption: (a) MW-HA, (b) DZ-HA, (c) HM-HA, and (d) C-HA (T = 25 °C, pH = 5, ionic strength = 0 mol L^{-1}).

contacting with the HA. The values of the rate constant k_2 of HAs were found to decrease with the increase in C_0 from 50 to 200 μg L^{-1}. It indicates that the adsorption of higher concentration of U(VI) to a specific removal percentage would take a longer time.

The adsorption capacity q_e(exp) of the MW-HA, DZ-HA, HM-HA, and C-HA at $C_0 = 100$ μg/L are 0.87, 0.28, 1.18 and 1.63 mg g^{-1}, respectively. However, the uranium concentration of the MW-HA and DZ-HA are 66.91 and 19.92 mg kg^{-1}, respectively. It shows that the higher concentration of uranium present in the HA does not affect its adsorption capacity. In the pseudo-second-order model, the chemical reaction is crucial in the rate-limiting step. Differences in adsorption capacity and equilibrium time in different HAs may be caused by the number of carboxylic acid and phenolic hydroxyl functional groups.

Adsorption isotherm

The adsorption isotherms of U(VI) onto the HAs are shown in Table 5. The correlation coefficient indicates that the Langmuir and Freundlich model can be used to describe the experimental data. Jaynes (1991) revealed that the adsorption conforms to the Langmuir and Freundlich models when the value of r^2 is larger than 0.89.

The Langmuir isotherm was used to estimate the sorption capacity and K_L. According to the hypothesis of the Langmuir model, the U(VI) adsorbed on some sites of the HAs, whose binding energies are the same, and the process is single molecular layer adsorption. The sorption capacity, Q_m, of each HA increases with the uplifting of temperature, which indicates that raising temperature is beneficial to the adsorption process. The experimental data also fit well with

Table 4 | Calculated and experimental q_e values and r^2 of three models (T = 25 °C, pH = 5, I = 0 mol L^{-1})

			First-order equation			Pseudo-second-order equation			Intraparticle diffusion model		
HAs	C_0 (μg/L)	q_e(exp)	q_{e1}(cal)	k_1 (×10^{-2})	r^2	q_{e2}(cal)	k_2 (×10^{-2})	r^2	k_3 (×10^{-2})	C	r^2
MW-HA	50	0.43	0.42	2.32	0.8855	0.46	7.27	0.9282	1.36	0.14	0.7179
	100	0.87	0.74	2.75	0.8855	0.84	3.92	0.9127	2.65	0.24	0.7274
	200	1.37	1.29	3.45	0.8744	1.40	3.70	0.9369	3.64	0.58	0.6852
DZ-HA	50	0.21	0.20	1.10	0.9175	0.23	5.32	0.9304	0.81	0.02	0.8424
	100	0.28	0.26	1.19	0.9622	0.30	4.46	0.9782	1.03	0.03	0.8781
	200	0.84	0.78	1.16	0.9141	0.91	1.41	0.9351	3.20	0.09	0.8552
HM-HA	50	0.55	0.51	3.33	0.8029	0.56	8.61	0.9257	1.59	0.21	0.8474
	100	1.18	1.06	3.00	0.8524	1.18	3.39	0.9420	3.58	0.39	0.8054
	200	1.98	1.81	3.50	0.7912	1.96	2.67	0.9127	5.30	0.81	0.7971
C-HA	50	0.82	0.75	5.85	0.8671	0.83	9.47	0.9462	1.99	0.41	0.6038
	100	1.63	1.47	4.69	0.8411	1.61	4.03	0.9264	4.13	0.73	0.6357
	200	3.22	3.00	5.06	0.8895	3.27	2.16	0.9771	8.05	1.55	0.6641

Note: q_e(exp), q_{e1}(cal) and q_{e2}(cal) are in mg g^{-1}.

Table 5 | The Langmuir and Freundlich isotherms parameters for HAs adsorbents onto U(VI) (T = 25, 45 °C, pH = 5, I = 0 mol L^{-1})

		Langmuir isotherm			Freundlich isotherm		
HAs	T(°C)	Q_m	K_L	r^2	n	K_F	r^2
MW-HA	25	3.50	7.56	0.9887	1.56	6.36	0.9936
	45	5.74	8.38	0.9873	1.48	12.30	0.9792
DZ-HA	25	2.88	2.84	0.9837	1.30	3.61	0.9718
	45	3.31	3.22	0.9871	1.33	4.38	0.9762
HM-HA	25	5.62	9.97	0.9897	1.56	12.25	0.9867
	45	7.80	11.44	0.9947	1.47	20.98	0.9792
C-HA	25	8.08	12.04	0.9626	1.55	20.38	0.9799
	45	9.07	13.18	0.9698	1.52	25.28	0.9877

Note: K_L and K_F are in L mg^{-1}, Q_m is in mg g^{-1}, n is in g L^{-1}.

the Freundlich model, which reveals that some other sorption sites are non-uniform, and the value of $n > 1$ indicates the adsorption is a favorable process (Khalili & Al-Banna 2015).

The isotherm experiment data fitting the Langmuir and Freundlich models well demonstrate that both single molecular layer adsorption and heterogeneous surface conditions exist at the same time. The adsorption of U(VI) by the HAs extracted from the lignites involve more than one mechanism.

Desorption studies

The adsorption and desorption are reversible processes, and the adsorbed metal ions can be desorbed under certain conditions. The desorption efficiency can be used to illustrate the binding degree of HA and metal ions. NH_4Ac was used as the desorption agent to represent the cations adsorbed onto the HA by ion-exchange effect. The desorption amount of the metal ions by EDTA suggests that metal ions adsorbed onto HA is determined by complexation effect and ion-exchange effect.

Different concentrations of NH_4Ac and EDTA were used as eluting agents for the removal of uranium from the HAs; the results are presented in Figure 7. It is clear that when the concentration of NH_4Ac and EDTA increased, the desorption efficiency of uranium increased. The maximum desorption percentages of uranium from the MW-HA, DZ-HA and HM-HA in EDTA solution are 51.32%, 66.21% and 54.78%, and in NH_4Ac solution are 12.22%, 5.24% and 9.74%. It indicates that the uranium adsorption onto the MW-HA, DZ-HA and HM-HA is controlled by the complexation with the organic ligands, and the effect of ion exchange was not the main adsorption mechanism. The results of uranium desorption from the C-HA are not identical to the other three kinds of HAs. The maximum desorption percentage of uranium from C-HA in NH_4Ac and EDTA solution are 19.17% and 44.29%, which may suggest that both the complexation and ion-exchange effect are the control factors for the adsorption of uranium onto the C-HA.

CONCLUSION

In this work, the characteristics of three different HAs extracted from uranium-enriched lignites and one

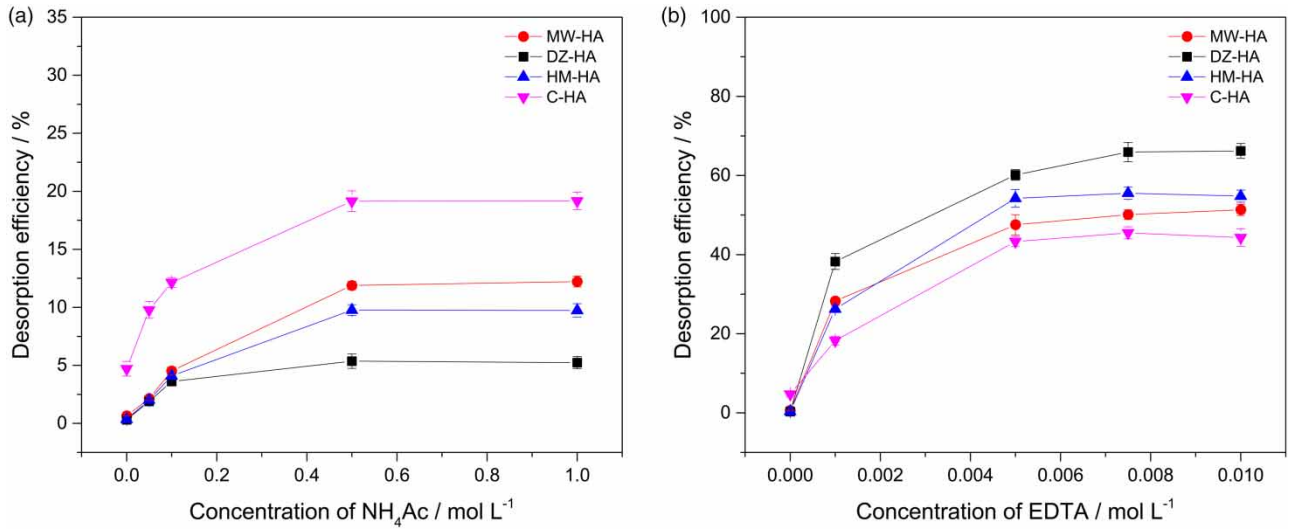

Figure 7 | Desorption efficiency of uranium under the effect of NH_4Ac and EDTA.

commercial HA were confirmed by elemental analysis, FTIR, determination of HAs acidity and UV-Vis spectroscopy. The adsorption of U(VI) onto the HAs was examined under various experimental conditions. The effective desorption with two different eluting agents for the U(VI) was also studied.

The results demonstrate that the U(VI) sorption onto the HAs is highly dependent on pH, and the optimum pH level at which all the HAs adsorbed uranium(VI) ranged from 5 to 8. The high uranium content of the HAs (e.g. MW-HA) could release into the solution at the pH value between 1 and 3, which shows that the HAs derived from uranium-enriched lignites present a potential environmental risk when used in acidic conditions. The adsorption kinetics data were best modeled using a pseudo-second-order equation and indicate that chemisorption is the rate-controlling mechanism. The adsorption isotherms fit the Langmuir and Freundlich models well, and prove that both single molecular layer adsorption and heterogeneous surface conditions exist in the adsorption process. The desorption percentage of the MW-HA, DZ-HA, and HM-HA in EDTA is much larger than that in NH_4Ac, which illustrates the adsorption process is controlled by the complexation effect in these HAs. The uranium existing in the HAs may not affect the adsorption capacity of uranium(VI). The results of the chemical characterization of the HAs demonstrate that the carboxylic and phenolic hydroxyl groups or other functional groups play a significant role in controlling the adsorption capacity.

ACKNOWLEDGEMENTS

This work was partially supported by the National Natural Science Foundation of China (NSFC, No. 41572233). We thank the anonymous reviewers and editor for their constructive comments and suggestions, which helped us to improve the manuscript.

REFERENCES

Adamczuk, A. & Kołodyńska, D. 2015 Equilibrium, thermodynamic and kinetic studies on removal of chromium, copper, zinc and arsenic from aqueous solutions onto fly ash coated by chitosan. *Chemical Engineering Journal* **274**, 200–212. DOI:10.1016/j.cej.2015.03.088.

Ciarkowska, K., Solek-Podwika, K., Filipek-Mazur, B. & Tabak, M. 2017 Comparative effects of lignite-derived humic acids and FYM on soil properties and vegetable yield. *Geoderma* **303**, 85–92. DOI:10.1016/j.geoderma.2017.05.022.

Cihlář, Z., Vojtová, L., Conte, P., Nasir, S. & Kučerík, J. 2014 Hydration and water holding properties of cross-linked lignite humic acids. *Geoderma* **230–231**, 151–160. DOI:10.1016/j.geoderma.2014.04.018.

Cihlář, Z., Vojtová, L., Michlovská, L. & Kučerík, J. 2016 Preparation and hydration characteristics of carbodiimide crosslinked lignite humic acids. *Geoderma* **274**, 10–17. DOI:10.1016/j.geoderma.2016.03.009.

Dai, S., Ren, D., Zhou, Y., Chou, C., Wang, X., Zhao, L. & Zhu, X. 2008 Mineralogy and geochemistry of a superhigh-organic-sulfur coal, Yanshan Coalfield, Yunnan, China: evidence for a volcanic ash component and influence by submarine

exhalation. *Chemical Geology* **255** (1–2), 182–194. DOI:10.1016/j.chemgeo.2008.06.030.

Dai, S., Wang, X., Zhou, Y., Hower, J. C., Li, D., Chen, W., Zhu, X. & Zou, J. 2011 Chemical and mineralogical compositions of silicic, mafic, and alkali tonsteins in the late Permian coals from the Songzao Coalfield, Chongqing, Southwest China. *Chemical Geology* **282** (1–2), 29–44. DOI:10.1016/j.chemgeo.2011.01.006.

Ghabbour, E. A., Davies, G., Lam, Y. Y. & Vozzella, M. E. 2004 Metal binding by humic acids isolated from water hyacinth plants (*Eichhornia crassipes* [Mart.] Solm-Laubach: Pontedericeae) in the Nile Delta, Egypt. *Environmental Pollution* **131** (3), 445–451. DOI:10.1016/j.envpol.2004.02.013.

Hou, B., Keeling, J. & Li, Z. 2017 Paleovalley-related uranium deposits in Australia and China: a review of geological and exploration models and methods. *Ore Geology Reviews* **88**, 201–234. DOI:10.1016/j.oregeorev.2017.05.005.

Jaynes, W. F. 1991 Hydrophobicity of siloxane surfaces in smectites as revealed by aromatic hydrocarbon adsorption from water. *Advances in Applied Microbiology* **39** (4), 133–168. DOI:10.1346/CCMN.1991.0390412.

Jing, C., Li, Y., Cui, R. & Xu, J. 2015 Illite-supported nanoscale zero-valent iron for removal of 238U from aqueous solution: characterization, reactivity and mechanism. *Journal of Radioanalytical and Nuclear Chemistry* **304** (2), 859–865. DOI:10.1007/s10967-014-3850-2.

Kautenburger, R., Sander, J. M. & Hein, C. 2017 Europium (III) and uranium (VI) complexation by natural organic matter (NOM): effect of source. *Electrophoresis* **38** (6), 930–937. DOI:10.1002/elps.201600488.

Khalili, F. & Al-Banna, G. 2015 Adsorption of uranium(VI) and thorium(IV) by insolubilized humic acid from Ajloun soil – Jordan. *Journal of Environmental Radioactivity* **146**, 16–26. DOI:10.1016/j.jenvrad.2015.03.035.

Khalili, F. I., Khalifa, A. A. & Al-Banna, G. 2017 Removal of uranium(VI) and thorium(IV) by insolubilized humic acid originated from Azraq soil in Jordan. *Journal of Radioanalytical and Nuclear Chemistry* **311** (2), 1375–1392. DOI:10.1007/s10967-016-5031-y.

Klučáková, M. & Pekař, M. 2008 Behaviour of partially soluble humic acids in aqueous suspension. *Colloids and Surfaces A: Physicochemical and Engineering Aspects* **318** (1–3), 106–110. DOI:10.1016/j.colsurfa.2007.12.023.

Li, Y., Yue, Q. & Gao, B. 2010 Adsorption kinetics and desorption of Cu(II) and Zn(II) from aqueous solution onto humic acid. *Journal of Hazardous Materials* **178** (1–3), 455–461. DOI:10.1016/j.jhazmat.2010.01.103.

Li, Y., Zhuang, R., Zhang, Z., Zhao, W., Wang, P., Xia, J. & Li, G. 2015 Research on the structure, chemical composition and characterization of humic acid from lignite. *Chemical Industry and Engineering Progress* **34** (8), 3147–3157. DOI:10.16085/j.issn.1000-6613.2015.08.039.

Pehlivan, E. & Arslan, G. 2006 Comparison of adsorption capacity of young brown coals and humic acids prepared from different coal mines in Anatolia. *Journal of Hazardous Materials* **138** (2), 401–408. DOI:10.1016/j.jhazmat.2006.05.063.

Sun, Y., Wu, Z., Wang, X., Ding, C., Cheng, W., Yu, S. & Wang, X. 2016 Macroscopic and microscopic investigation of U(VI) and Eu(III) adsorption on carbonaceous nanofibers. *Environmental Science & Technology* **50** (8), 4459–4467. DOI:10.1021/acs.est.6b00058.

Wang, X., Wang, T., Zheng, X., Shen, Y. & Lu, X. 2017a Isotherms, thermodynamic and mechanism studies of removal of low concentration uranium (VI) by *Aspergillus niger*. *Water Science and Technology* **75** (12), 2727–2736. DOI:10.2166/wst.2017.055.

Wang, C. F., Fan, X., Zhang, F., Wang, S. Z., Zhao, Y. P., Zhao, X. Y., Zhao, W., Zhu, T. G., Lu, J. L. & Wei, X. Y. 2017b Characterization of humic acids extracted from a lignite and interpretation for the mass spectra. *RSC Advances* **7** (33), 20677–20684. DOI:10.1039/c7ra01497j.

World Health Organization 2011 *Guidelines for Drinking-Water Quality*, 4th edn. World Health Organization, Geneva, Switzerland.

Yang, J. 2007 Concentration and distribution of uranium in Chinese coals. *Energy* **32** (3), 203–212. DOI:10.1016/j.energy.2006.04.012.

Yue, Q., Li, Y. & Gao, B. 2009 Impact factors and thermodynamic characteristics of aquatic humic acid loaded onto kaolin. *Colloids and Surfaces B: Biointerfaces* **72** (2), 241–247. DOI:10.1016/j.colsurfb.2009.04.010.

Zhang, Y., Shi, M., Wang, J., Yao, J., Cao, Y., Romero, C. E. & Pan, W. 2016 Occurrence of uranium in Chinese coals and its emissions from coal-fired power plants. *Fuel* **166**, 404–409. DOI:10.1016/j.fuel.2015.11.014.

First received 12 September 2017; accepted in revised form 21 November 2017. Available online 1 December 2017